



**HAL**  
open science

## A distributed virtual MIMO coalition formation framework for energy efficient wireless networks

Rodrigo A Vaca Ramirez, John S Thompson, Eitan Altman, Victor Ramos

► **To cite this version:**

Rodrigo A Vaca Ramirez, John S Thompson, Eitan Altman, Victor Ramos. A distributed virtual MIMO coalition formation framework for energy efficient wireless networks. EURASIP Journal on Wireless Communications and Networking, 2015, 2015 (1), pp.1-21. 10.1186/s13638-015-0308-3 . hal-01152463

**HAL Id: hal-01152463**

**<https://inria.hal.science/hal-01152463>**

Submitted on 17 May 2015

**HAL** is a multi-disciplinary open access archive for the deposit and dissemination of scientific research documents, whether they are published or not. The documents may come from teaching and research institutions in France or abroad, or from public or private research centers.

L'archive ouverte pluridisciplinaire **HAL**, est destinée au dépôt et à la diffusion de documents scientifiques de niveau recherche, publiés ou non, émanant des établissements d'enseignement et de recherche français ou étrangers, des laboratoires publics ou privés.

# A Distributed Virtual MIMO Coalition Formation Framework for Energy Efficient Wireless Networks

Rodrigo A. Vaca Ramírez<sup>(1)</sup>, John Thompson<sup>(1)</sup>, Eitan Altman<sup>(2)</sup>, and Víctor M. Ramos R.<sup>(3)</sup>

<sup>(1)</sup>*The University of Edinburgh, Institute for Digital Communications,*

*King's Buildings, Mayfield Road, Edinburgh, EH9 3JL, UK.*

<sup>(2)</sup>*INRIA, Sophia Antipolis Cedex, BP93, 06902 France.*

<sup>(3)</sup>*Universidad Autónoma Metropolitana (UAM),*

*Department of Electrical Engineering Iztapalapa, Mexico City*

*E-Mail: {r.vaca, john.thompson}@ed.ac.uk, eitan.altman@inria.fr, vicman@xanum.uam.mx*

## Abstract

In this paper, we consider a low complexity virtual Multiple-input Multiple-output (MIMO) coalition formation algorithm. The goal is to obtain improvements in energy efficiency by forming multi-antenna virtual arrays for information transmission in the uplink. Virtual arrays are formed by finding a stable match between single antenna devices such as mobile station (MS) and relay stations (RS) by using a game theoretic approach derived from the concept of the college admissions problem. We focus on enhancing the mobile station (MS) performance by forming virtual coalitions with the RSs. Thus, power savings are obtained through multi-antenna arrays by implementing the concepts of spatial diversity and spatial multiplexing for uplink transmission. We focus on optimizing the overall consumed power rather than the transmitted power of the network devices. Furthermore, it is shown analytically and by simulations that when overall consumed power is considered as an optimization metric, the energy efficiency of the single antennas devices is not always improved by forming a virtual MIMO array. Hence, single antenna devices may prefer to transmit on their own when channel conditions are favorable. In addition, the simulation results show that our proposed framework provides comparable energy savings and a lower implementation complexity when compared to a centralized exhaustive search approach that is coordinated from the BS.

## Index Terms

Game theory; energy efficiency; cooperative communications; virtual MIMO.

## I. INTRODUCTION

Energy consumption has become a major research topic from environmental and economical perspectives due to the worldwide growth in the number of mobile subscribers which comes together with associated carbon emissions and growing energy costs. Moreover, the data volume of communication networks is expected to grow by a factor of ten every five years, which brings a doubling of energy consumption over the same time period [1–3]. Thus, academia and industry researchers have started to consider solutions to reduce energy consumption rather than just improve the network's capacity.

Use of multiple antennas in wireless links has emerged as an effective way to enhance the energy efficiency. It has been shown in [4] that multi-antenna systems require less transmitted power to achieve the same capacity requirements than single antenna devices. In Long Term Evolution (LTE), a base station (BS) may support multiple antennas. However, mobile stations (MSs) may not be equipped with more than one single antenna due to physical constraints [5, 6]. Hence, implementing effective solutions, that allow MSs to benefit from the advantages of multi-antenna systems without the extra burden of having multiple antennas physically present at the users' side, has become a major issue for current communication systems.

Cooperative communications have recently attracted significant attention as an effective way to improve the performance of wireless networks [7]. By the use of cooperative techniques wireless devices are allowed to share and utilize the network resources in a more efficient way [7–13]. As an example, the authors in [10] present a cooperative method to share the network resources and manage interference among femtocells in a distributed manner. Hence, femtocells form coalitions to improve their performance by sharing spectral resources and maximizing the spatial reuse. In [12], the authors consider the consequences that arise when two multi-antenna systems share the same spectrum band. They demonstrate that if cooperation between the two systems is possible, they may achieve a performance close to the max-sum-rate.

An important application of cooperative techniques is the formation of virtual multi-antenna arrays. In this context, a number of single antenna devices may cooperate with each other by forming virtual Multiple-input Multiple-output (MIMO) transmitters or receivers to reap some of the benefits of multi-antenna systems [14]. The theoretical aspects of virtual MIMO have previously been covered in [14, 15]. Virtual MIMO literature which considers energy efficiency as an optimization constraint can be found in [5, 8, 16]. The authors in [16, 17] illustrate the energy savings obtained when virtual MIMO techniques

are used compared with non-cooperative approaches in wireless sensor networks. They argue that at certain distance ranges from the destination node, cooperative MIMO results in a more energy efficient solution that also reduces the total delay compared with no-cooperation. In [5], an approach to optimize the power allocation between transmitter and relay in order to minimize the overall energy per bit consumption in the system is presented. Moreover, it is shown that by using an optimal power allocation, the virtual MIMO case achieves an energy efficiency performance close to the ideal MIMO system.

As mentioned previously, most of the current research in energy efficient virtual MIMO tackles the problem of “why to cooperate”. Nevertheless, there are two questions that remain unanswered “when to cooperate” and “with whom to cooperate”. In this work we aim to provide an answer for both questions by providing a coalition formation framework that allows single antenna devices to decide with whom to cooperate in order to obtain energy savings in the reverse link transmission.

In addition, the implementation of cooperative solutions may face many challenges due to the large scale nature of wireless systems. Cooperation comes along with costs such as power expenditure that may limit or reduce the system’s performance. Moreover, if cooperation between the users is regulated by a centralized entity, a significant amount of wireless signaling overhead is required between the users and the network. Furthermore, it is well known that the use of centralized techniques entails extra implementation costs and an increase in system’s complexity [1, 18, 19]. Thus, the design of effective techniques that allows the single antenna devices to *autonomously* decide when and with whom to cooperate is a matter of vital importance for current networks [20]. In this regard, game theory provides a powerful mathematical tool for the design of distributed solutions in cooperative communications [7, 9, 20, 21]. Through the use of coalitional game theory, the authors in [20] propose a merge and split distributed algorithm to form multi-antenna coalitions among single antenna devices. The aim of their work is to maximize the users’ rate while accounting for the cost of cooperation in terms of power. In [21], we propose an energy efficient solution for virtual MIMO coalition formation, where cooperation is modeled as a game theoretical approach derived for the concept of stable marriage with incomplete lists. An optimal relay is selected to minimize the reverse link power expenditure. Furthermore, we show that the communication overhead can be reduced significantly if distributed techniques are used. Nevertheless, a major drawback of the proposed framework in [21] is that the number of elements that can join the coalition is constrained to a limited number.

The main contributions of this paper are: (1) to provide a distributed low complexity virtual MIMO coalition formation algorithm for energy efficient networks; (2) our proposed solution can support any number of transmitters participating in the coalitions; (3) we focus on enhancing the mobile station (MS)

performance by forming virtual coalitions with the RSs; (4) we analyze our proposal from both diversity and capacity perspectives; (5) the proposed solution focuses on reducing the overall consumed power rather than the transmitter power, thus the power consumption of the radio frequency (RF) parts such as the power amplifiers and the base band (BB) module is taken into account.

The rest of the paper is structured as follows: Section II describes the problem scenario, Section III presents our power consumption model and performance metrics. In Section IV, our cooperative framework is shown. Moreover, in Section V we present a theoretical analysis of the consequences arising when optimizing overall consumed power rather than transmitted power when implementing spatial diversity and spatial multiplexing in multi-antenna systems. A summary of the comparison schemes and our simulation scenario is described in Section VI. Simulation results are presented in Section VII. Finally, Section VIII offers concluding remarks.

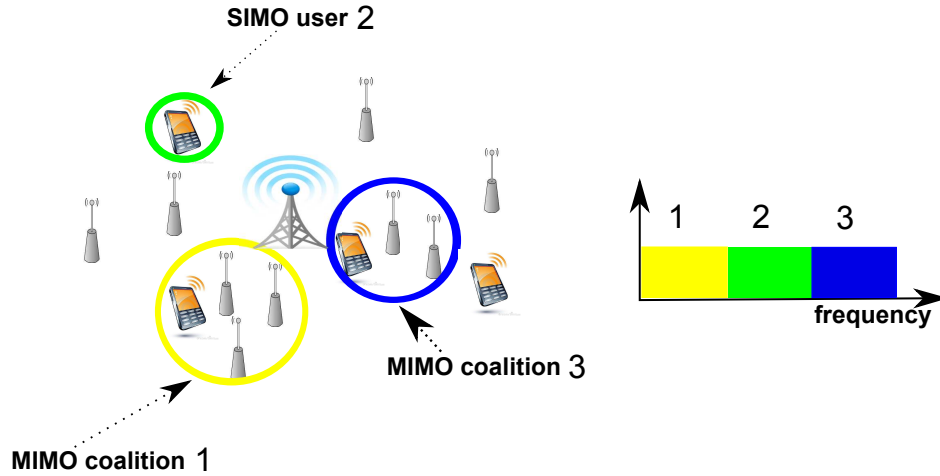
## II. SYSTEM SCENARIO

In this section, the scenario adopted in this paper is described. We consider a system with  $N$  single antenna mobile stations (MSs) that transmit data to a multi-antenna base station. In addition,  $R$  single antenna relay stations (RSs) are uniformly distributed through the cell, assuming  $R \gg N$ . In order to improve the user's performance, single antenna devices (MSs and RS) are allowed to cooperate by forming virtual  $M_t \times M_r$  MIMO coalitions, where  $M_r$  is the number of antennas at the base station (BS), and  $M_t$  is the number of single antenna devices forming a virtual MIMO link. If cooperation is not feasible, MSs will prefer to transmit to their own to the BS in Single-input Multiple-output (SIMO) mode.

In Fig. 1 the orthogonal frequency division multiple access (OFDMA) scenario is shown, the system bandwidth  $B$  (Hz) is divided into  $X$  resource blocks (RBs). Each RB is assigned to each user independently to avoid mutual interference. An RB defines the basic time-frequency unit with bandwidth  $B_{RB} = B/X$  (Hz).

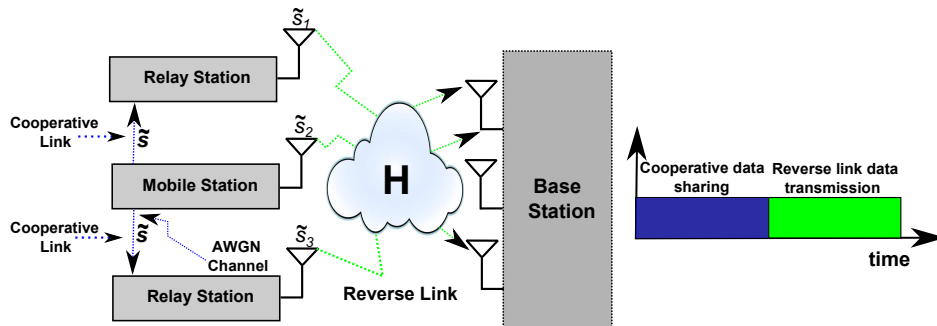
### A. Virtual MIMO Link

Fig. 2 shows a virtual  $M_t \times M_r$  MIMO link that implements spatial multiplexing. At the first time slot, the MS forwards the information vector  $\mathbf{s}$  to its peers by using the cooperative link. In the following slot the MS and RSs will transmit the information vector  $\mathbf{s}$  at the reverse link through the MIMO channel  $\mathbf{H}$ . In addition, to avoid mutual interference the reverse and the cooperative link should be designed orthogonal to each other. When spatial multiplexing is implemented, we assume that the cooperative link



**Fig. 1** User cooperation example coalitions considering an OFDMA transmission model.

is fast enough on information transmission, thus MSs can transmit their signal vector  $\mathbf{s}$  to the cooperating peers and they can demultiplex it into independent information streams for simultaneous transmission. A similar representation can be used for the spatial diversity concept by replacing the vector  $\mathbf{s}$  by the information symbol  $s$ . Thereby, all antennas involved in the coalition transmit the same symbol  $s$  in the reverse link.



**Fig. 2** A Virtual  $M_t \times M_r$  MIMO link.

### B. Cooperative Link

For the single antenna devices (MSs and RSs) to cooperate among each other, the set up and maintenance of a cooperative link is required. The cooperative link is based on a short range transmission, which is primarily used for information exchange between the transmitting peers. Thus, the channel between the

MS- $n$  and the RS- $r$  can be modeled as a  $\kappa^{th}$ -power path loss (loss  $\approx \frac{1}{l_{nr}^\kappa}$ ) with Additive White Gaussian Noise (AWGN). Accordingly, the received power  $P_{nr}$  at the RS- $r$ , transmitted from the MS- $n$  is given by:

$$P_{nr} = P_{tnr} l_{nr}^{-\kappa} \quad (1)$$

where  $l_{nr}$  is the distance between the RS- $r$  and the MS- $n$ , and  $P_{tnr}$  is the transmitted power for cooperation. Hence, the signal-noise ratio (SNR) at the RS side is represented by

$$\eta_{nr} = \frac{P_{nr}}{\rho}. \quad (2)$$

Moreover, due to the broadcast nature of the wireless channel, when the MS broadcasts its information to the farthest RS in the coalition, all other RSs can also receive and decode this information simultaneously. Thus, define  $S'_n \in R$  as the subset of RSs which have formed a coalition with the MS- $n$ . The cost of cooperation can be defined as the MS's maximum transmitted power spend to reach the farthest RS in the coalition. Thereby, define the set of distances between the MS- $n$  and its  $S'_n$  subset of RSs as

$$\begin{aligned} D_{nr}^* &= \{l_{n(1)}, l_{n(2)}, \dots, l_{n(N)}\}, \\ \text{s.t } l_{n(1)} &\leq l_{n(2)} \leq \dots \leq l_{n(N)}, \end{aligned} \quad (3)$$

where  $N = |S'_n|$ , and  $|\cdot|$  defines the cardinality of the sub-set. Thus, the power spent for cooperation may be represented by

$$P_{\text{tcoop}} = \eta_{n(N)} l_{n(N)}^\kappa \rho. \quad (4)$$

### C. Reverse link channel model

The channel coefficient between a multi-antenna BS separated by a distance  $l_k$  from the  $k$ -th MIMO coalition is determined by path loss, log-normal shadowing, and channel variations caused by frequency selective fading. In this work, a fading Rayleigh channel is considered, thus the fading coefficients for an  $M_t \times M_r$  MIMO channel can be represented by a matrix

$$\mathbf{H} = \begin{bmatrix} h_{1,1} & h_{1,2} & \cdots & h_{1,M_t} \\ h_{2,1} & h_{2,2} & \cdots & h_{2,M_t} \\ \vdots & \vdots & \ddots & \vdots \\ h_{M_r,1} & h_{M_r,2} & \cdots & h_{M_r,M_t} \end{bmatrix}, \quad (5)$$

where each matrix element defines a Zero Mean Circular Symmetric Complex Gaussian (ZMCSCG) random variable with unit variance [4]. If the MS prefers to transmit in SIMO mode the channel can be

defined by the following vector:

$$\mathbf{h} = [h_1, h_2, \dots, h_{M_r}]^T. \quad (6)$$

Furthermore, path loss and shadowing are considered as a power fall off that attenuates the transmitted signal, thus, the received power  $P_r$  at the BS side is given by [22]

$$P_r = P_t 10^{\frac{-L(l_k) + X_\sigma}{10}}, \quad (7)$$

where  $P_t$  represents the transmitted power,  $X_\sigma$  is the log-normal shadowing value (dB) with standard deviation  $\sigma$ , and  $L(l_k)$  is the distance dependent path loss (dB) which is calculated as follows:

$$L(l_k) = a + b \log_{10}(l_k) \text{ [dB]}. \quad (8)$$

where  $a = 15.3$  and  $b = 37.6$  are pathloss constants for a micro urban cell scenario. Moreover, since, single antenna devices utilize a short range transmitter for information exchange, a valid assumption is to consider that the elements involved in a MIMO coalition are sufficiently closely spaced to experience the same channel statistics. Thereby, shadowing and path loss remain the same for the devices forming a virtual link. In addition, the receiver and transmitter are assumed to know the channel coefficients between them. State of the art wireless standards such as LTE may implement closed loop techniques to obtain current channel state information [23]. In this work, coalitions are formed to reduce the reverse link power consumption by using the concepts of spatial diversity and spatial multiplexing as shown below.

1) *Spatial diversity*: The received signal at the BS from the  $k$ -th MIMO coalition is represented as:

$$\mathbf{y}_k = \sqrt{\frac{P_r}{M_t}} \mathbf{H} \mathbf{w} s + \mathbf{n}, \quad (9)$$

where  $M_t$  is the number of transmit antennas per *coalition*,  $s$  is the scalar information symbol with unit energy,  $\mathbf{n}$  is the noise, and  $\mathbf{w}$  is a complex weight vector that should satisfy  $\|\mathbf{w}\|_F^2 = M_t$  to constrain the total average transmitted power, where  $\|\cdot\|_F^2$  is the Frobenius norm.

Accordingly, the signal-to-noise ratio (SNR) for a MIMO coalition is given by [4]:

$$\eta_{k\_mimo} = \frac{\|\mathbf{g}^H \mathbf{H} \mathbf{w}\|_F^2 P_r}{M_t \|\mathbf{g}\|_F^2 \rho}, \quad (10)$$

where  $\rho$  is the noise power and  $\mathbf{g}$  is an  $M_r \times 1$  complex weight vector which multiplies the received signal at the BS. Thus, maximizing the SNR at the receiver side is equivalent to maximizing the term  $\|\mathbf{g}^H \mathbf{H} \mathbf{w}\|_F^2 / \|\mathbf{g}\|_F^2$ . The proper choices of  $\mathbf{w}/\sqrt{M_t}$  and  $\mathbf{g}$  that maximize the SNR are the input and output



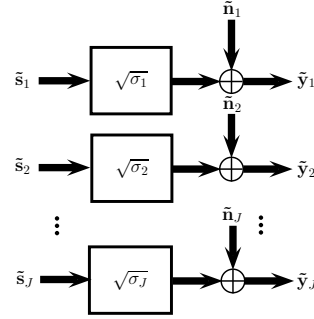


**Fig. 3** Modal decomposition of the channel.

singular value vectors corresponding to the maximum singular value  $\sigma_{max}$  of  $\mathbf{H}$  [4]. By the use of the singular value decomposition (SVD) the channel matrix can be represented as  $\mathbf{H} = \mathbf{U}\Sigma\mathbf{V}^H$ , where  $\mathbf{V}^H$  represents the conjugate transpose of  $\mathbf{V}$ . Moreover, the columns of  $\mathbf{V}$  and  $\mathbf{U}$  are known as the input and output singular vectors respectively. In addition  $\Sigma = \text{diag}\{\sigma_1, \sigma_2, \dots, \sigma_J\}$  with  $\sigma_i \geq 0$ , where  $\sigma_i$  is the  $i$ -th singular value of the channel, and  $J$  is the rank of  $\mathbf{H}$ . Thus, the received SNR at the BS side from the  $k$ -th MIMO coalition may be expressed as follows:

$$\eta_{k\_mimo} = \frac{\sigma_{max}^2 P_r}{\rho}, \quad (11)$$

In the case of a SIMO user, Eq. (9) is re-written in the following way:

$$\mathbf{y}_k = \sqrt{P_r} \mathbf{h} \mathbf{s} + \mathbf{n}. \quad (12)$$

Thereby, the received SNR at the BS may be represented by [4]:

$$\eta_{k\_simo} = \frac{\|\mathbf{h}\|_F^2 P_r}{\rho}, \quad (13)$$

2) *Spatial Multiplexing*: When channel knowledge is assumed, the individual spatial channel modes may be accessed through linear processing at the transmitter and receiver side [4]. Thus, a signal vector  $\mathbf{s}$  of dimension  $J \times 1$  which is transmitted from the  $k$ -th MIMO coalition through a  $J$  rank MIMO channel,  $\mathbf{H}$ , after linear processing at the BS side is represented by:

$$\begin{aligned} \tilde{\mathbf{y}}_k &= \sqrt{\frac{P_r}{M_t}} \mathbf{U}^H \mathbf{H} \mathbf{V} \mathbf{s} + \mathbf{U}^H \mathbf{n}, \\ &= \sqrt{\frac{P_r}{M_t}} \Sigma \mathbf{s} + \tilde{\mathbf{n}} \end{aligned} \quad (14)$$

where  $\mathbf{V}$  represents the matrix with dimensions  $M_t \times J$  that multiplies  $\mathbf{s}$  at the transmitter side. Moreover,  $\mathbf{U}^H$  represents the matrix with dimensions  $M_r \times J$  that multiplies the signal at the receiver side. In addition  $\tilde{\mathbf{n}}$  is the ZMCSCG noise vector after processing, with dimensions  $J \times 1$ . The transmitted signal vector  $\mathbf{s}$  must satisfy:  $\mathbf{E}\{\mathbf{s}\mathbf{s}^H\} = M_t$ , to constrain the total transmitted power. Furthermore, Fig. 3 shows how  $\mathbf{H}$  is decomposed into  $J$  parallel SISO channels under the assumption of channel knowledge at the transmitter side, where each parallel sub-channel satisfies

$$\tilde{y}_i = \sqrt{\frac{P_r}{M_t}} \sqrt{\sigma_i} s_i + \tilde{n}_i, \quad i = 1, 2, \dots, J. \quad (15)$$

Hence, the total uplink user throughput will become the sum of the individual parallel SISO channels capacities, where the SNR of the  $i$ -th spatial channel (SC) is given by

$$\eta_{i\_SC} = \frac{P_r \zeta_i \sigma_i}{M_t \rho}, \quad (16)$$

where  $\zeta_i = \mathbf{E}\{\|\mathbf{s}_i\|^2\}$   $i = 1, 2, \dots, J$ , represents the transmitted power in the  $i$ -th SISO parallel sub-channel and must satisfy  $\sum_{i=1}^J \zeta_i = M_t$ .

Furthermore, since the transmitter may access the multiple parallel SISO channels, the problem becomes how to allocate the power in an way that maximizes the mutual information. The optimal value of  $\zeta_i$  is found iteratively through the use of the water-pouring method, which is explained in detail in [24]. When cooperation is not suitable, the MSs will transmit in SIMO mode, where the achievable SNR is defined by Eq. (13).

### III. PHYSICAL COMPONENTS POWER CONSUMPTION MODEL AND PERFORMANCE METRICS FOR OPTIMIZING OVERALL CONSUMED POWER

In this paper, we focus on optimizing the overall power consumption of the MS's components rather than only the transmitted power. For the MIMO user case, we consider the power expenditure in the reverse and the cooperative link. When cooperation is not feasible, MSs would prefer to transmit in SIMO mode, hence only the reverse link power expenditure is only taken into account. The reverse and cooperative link power consumption mainly depend on components such as the radio frequency (RF) parts and the base-band (BB) signal processing module [25]. The RF module incorporates the power expenditure of power amplifiers for transmission. Moreover, the BB module comprises the power consumption for channel coding/decoding and modulation/demodulation. For modeling the RF and BB module, we use the model previously presented in [25], where the authors make an analysis of the power expenditure for both modules in a Long Term Evolution (LTE) mobile station. Therefore, the overall

consumed power in SIMO mode,  $P_{\text{simo}}$ , depends primarily on the transmitted power in the uplink  $P_t$ .

$$P_{\text{simo}}(P_t) = P_{\text{circ}}(P_t) \quad (17)$$

Furthermore, the total consumed power to form a virtual MIMO link becomes a function of the transmitted power in the reverse link  $P_t$ , and how this is distributed between the mobile and the relay stations, which is defined by the weight vector,  $\mathbf{w}$ , when implementing spatial diversity and by the water filling coefficients  $\zeta_i$   $i = 1, 2, \dots, J$  for the spatial multiplexing case. Thus, the total consumed power in the uplink when implementing spatial diversity or spatial multiplexing respectively is obtained as follows:

$$P_{\text{mimo\_diversity}}(P_t) = \sum_{i=1}^{M_t} P_{\text{circ}} \left( \frac{P_t \|w_i\|^2}{M_t} \right) \quad (18)$$

$$P_{\text{mimo\_capacity}}(P_t) = \sum_{i=1}^{M_t} P_{\text{circ}} \left( \frac{P_t \zeta_i}{M_t} \right) \quad (19)$$

where  $P_{\text{circ}}$  defines the circuit power in the reverse link spent by each of single antenna device such as MSs or RSs forming the MIMO link. In addition, the power expenditure due to the cooperative link,  $P_{\text{circop}}$ , should be added to Eqs.(18) and (19). Thereby, the total power expenditure to form the virtual MIMO link when implementing spatial diversity or spatial multiplexing is given by:

$$P_{\text{mimo\_diversity\_total}}(P_t, P_{\text{tcop}}) = P_{\text{circop}}(P_{\text{tcop}}) + \sum_{i=1}^{M_t} P_{\text{circ}} \left( \frac{P_t \|w_i\|^2}{M_t} \right) \quad (20)$$

$$P_{\text{mimo\_capacity\_total}}(P_t, P_{\text{tcop}}) = P_{\text{circop}}(P_{\text{tcop}}) + \sum_{i=1}^{M_t} P_{\text{circ}} \left( \frac{P_t \zeta_i}{M_t} \right) \quad (21)$$

To model the circuit consumed power of the RF module, we consider a power amplifier array [25, 26] which is based on four power amplifiers: a low power amplifier (LPA) and three high power amplifiers HPA 1, HPA 2 and HPA 3 as presented in Fig 4. The power amplifier efficiency is assumed equal for both high power amplifiers; however HPA 1 and 2 are designed to transmit up to one fourth and to one half of the maximum transmitted power of HPA 3 respectively. Thus, the circuit power expenditure at the uplink  $P_{\text{circ}}$  [W] is given by:

$$P_{\text{circ}}(P_t^*) = \begin{cases} 2 + 0.005(P_t^*) - A & 14 \geq P_t^* \\ \frac{1.2 + 0.12(P_t^*) - (A - \frac{3}{4}P_{BB})}{4} & 17 \geq P_t^* > 14 \\ \frac{1.2 + 0.12(P_t^*) - (A - P_{BB})}{2} & 20 \geq P_t^* > 17 \\ 1.2 + 0.12(P_t^*) - A & 24 \geq P_t^* > 20 \end{cases} \quad (22)$$

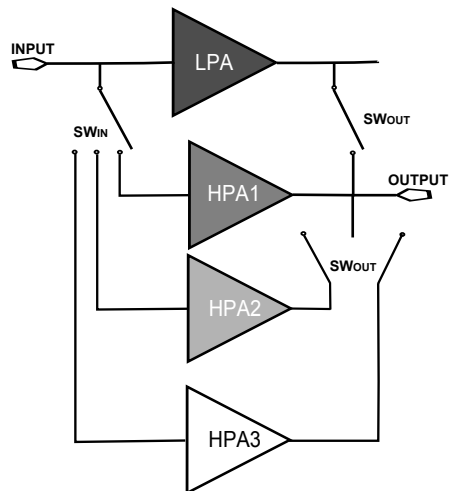


**Fig. 4** Internal model of the power amplifier for the RF module.

where the  $P_t^*$  represents the transmitted power per antenna in [dBm], which is the input value converted to [dBm] of  $P_{\text{circ}}$  in Equations (17), (20), (21), and  $A$  is a set of constant values defined as follows [25]:

$$A = P_{T_x} + P_{\text{con}} - P_{BB} \text{ [W]}, \quad (23)$$

The value  $P_{T_x}$  is the minimum power that the RF chain consumes in transmission mode,  $P_{\text{con}}$  is the MS's power consumption when connected to the BS, and  $P_{BB}$  is the power consumed by the BB module [25].

In addition, the cooperative link is constructed by using a short range communications link, thus to model its circuit power expenditure  $P_{\text{circop}}$ , we use the LPA model shown below:

$$P_{\text{circop}}(P_{\text{tcop}}) = 2 + 0.005(P_{\text{tcop}}) - A \text{ [W]} \quad 14 \geq P_{\text{tcop}} \text{ [dBm]} \quad (24)$$

#### A. Performance Metrics to Optimize Circuit Consumed Power

The achievable throughput on the link between the  $k$ -th coalition and the BS when diversity is enhanced is calculated as [22]:

$$T_{k\_diversity}(\eta_k) = n_k^{RB} k_{sc} \varrho_s \varepsilon(\eta_k) \text{ [bits/s]}, \quad (25)$$

where  $n_k^{RB}$  is the number of resource blocks assigned to the  $k$ -th coalition,  $k_{sc}$  is the number of subcarriers per resource block,  $\varrho_s$  is the symbol rate per subcarrier, and  $\varepsilon(\eta_k)$  is the spectral efficiency for a LTE system [22]. Moreover,  $\eta_k$  in (25) must be replaced by (11) when the user transmits in MIMO or by

(13) when the user transmits in SIMO mode. In the case when spatial multiplexing is implemented, the throughput is given by:

$$T_{k\_capacity}(\eta_{i\_SC}) = n_k^{RB} k_{sc} \rho_s \sum_{i=1}^J \varepsilon(\eta_{i\_SC}) \text{ [bits/s]}, \quad (26)$$

where  $\eta_{i\_SC}$  is the SNR in the  $i$ -th individual parallel SISO channel previously given in (16) and  $J$  is defined as the rank of the channel. The user energy efficiency  $\beta_k$  measures the user throughput per unit of consumed energy.

$$\beta_k = T_k / P_{total\_k} \text{ [bits/J]}. \quad (27)$$

This is based on the total consumed power  $P_{total\_k}$ , where  $P_{total\_k}$  is equal to  $P_{simo}$  in (17) when the coalition acts in SIMO mode, and to  $P_{mimo\_diversity\_total}$  in (20) or  $P_{mimo\_capacity\_total}$  in (21), when a virtual MIMO link is constructed to implement spatial diversity or spatial multiplexing respectively. Moreover,  $T_k$  is replaced as required by  $T_{k\_diversity}$  in (25) or  $T_{k\_capacity}$  in (26). Additionally, the system energy efficiency  $\beta_{sys}$  is defined as the ratio between the total user throughput and the total power spent by all the users in the system:

$$\beta_{sys} = \frac{\sum_{k=1}^N T_k}{\sum_{k=1}^N P_{total\_k}} \text{ [bits/J]}. \quad (28)$$

#### IV. COLLEGE ADMISSION FRAMEWORK FOR DISTRIBUTED VIRTUAL MIMO COALITION FORMATION

In this paper, cooperation is modeled using a game theory approach derived from the college admissions problem [27]. The college admission framework (CAF) is used to find a stable match between two sets of elements (MSs and RSs). The CAF is a generalization of the stable marriage (SM) problem [28]. However, coalitions are not limited only to two participants as it happens in the SM case [21]. As described in [27], the CAF involves a set of colleges and a set of applicants. Each applicant lists in order of preference those institutions she/he aims to attend while each institution lists in order of preference those applicants it is willing to admit. Additionally, each institution has a limit in the number of applicants that is able to admit. Thus, the problem becomes to assign applicants to institutions in a way that takes into account both preferences and constraints. In our problem, the  $N$  MSs take the role of colleges and the  $R$  RSs become the applicants. Hence, RSs are assigned to MSs to form virtual MIMO coalitions with the aim of reducing the total energy consumption of the MSs. This case is studied in order to reduce the power consumption by allowing coalitions to implement spatial diversity or spatial multiplexing, respectively. An important property of the CAF is that it leads the system to a stable solution as described in [29]. Stability means that there are no RSs and an MSs in the system such that both of the following assumptions are true:

- The RS is unmatched or would prefer to form a virtual MIMO link with a different MS to the one that is currently matched with;
- The MS is able to include another RS into its MIMO coalition or would prefer to cooperate with a different RS to one of its current partners RSs.

A mapping  $M$  is a tuple of one MS with a subset of one or more RSs, such that each single antenna device (MS or RS) belongs exactly to one tuple. Hence, if  $(n, S'_n) \in M$ , we say that the  $S'_n$  subset of RSs is the cooperative partner set of MS- $n$  in  $M$  and vice versa, where  $S'_n \in R$ . The distributed coalition formation algorithm is described as follows:

- 1) At the beginning of the algorithm, each MS in the system sends a broadcast message through the cooperative link to find the subset of RSs willing to cooperate and form a virtual MIMO link, which for the MS- $n$  is denoted by  $S_n \in R$ .
- 2) Moreover, the RSs in the system exchange their channel statistics in the uplink (fading coefficient, path-loss and shadowing) and the channel statistics in the cooperative link (path loss) with the subset of MSs willing to cooperate with them, which for the RS- $r$  is denoted by  $S_r \in N$ . Thereafter, each mobile station has the means to rank its subset of suitable RSs,  $S_n$ , by using the following utility function, that in the diversity enhancement case is defined by:

$$U_{nr\_diversity}(\eta_{\text{target}}) = P_{\text{simo}}(\eta_{\text{target}}) - P_{\text{mimo\_diversity}}(\eta_{\text{target}}), \quad (29)$$

where  $U_{nr\_diversity}$  represents the difference in power expenditure when the MS- $n$  transmits at its own or forms a virtual MIMO link with the RS- $r$ , and  $\eta_{\text{target}}$  is a fix target SNR that SIMO and MIMO coalitions aim to achieve. Thus, the higher is the value of the utility, the more MS- $n$  will be willing to form a virtual link with RS- $r$ . Moreover, a negative value of  $U_{nr\_diversity}$  means that forming a coalition with the RS- $r$  become less energy efficient, thus the MS will prefer to transmit in SIMO mode. In the case when implementing spatial multiplexing, each MS- $n$  ranks each RS- $r$  from its subset  $S_n$  by using the following utility function:

$$U_{nr\_capacity}(T_{\text{target}}) = P_{\text{simo}}(T_{\text{target}}) - P_{\text{mimo\_capacity}}(T_{\text{target}}), \quad (30)$$

where  $U_{nr\_capacity}$  represents the difference in energy efficiency performance when the MS- $n$  transmits on its own or forms a coalition with RS- $r$ , and  $T_{\text{target}}$  represents a target transmission rate that both SIMO and MIMO users aim to achieve. Thus, as in the case where diversity is enhanced, the higher is the value of the utility the MS- $n$  will be more willing to form a virtual MIMO link with the RS- $r$ . The MS- $n$ 's preference list  $\iota_n$  is formed by evaluating each RS in  $S_n$  by using Eq.

(29) when diversity is enhanced or (30) for the capacity enhancement case. Moreover, the RSs of the MS- $n$ 's preference list,  $\iota_n$ , must be sorted in descending order as follows:

$$\begin{aligned} \iota_n &= \{\text{RS}_{n(h)}, \text{RS}_{n(2)}, \dots, \text{RS}_{n(1)}\}, \\ \text{s.t } U_{n(1)} &\leq U_{n(2)} \leq \dots \leq U_{n(h)}, \end{aligned} \quad (31)$$

where  $U_{n(r)}$  represents the pairwise comparisons between the MS- $n$  and the RS- $r$  which can be replaced by the values obtained from Eq. (29) or (30) whenever the preference list is designed for implementing spatial diversity or spatial multiplexing respectively. Notice that when the value of  $U_{n(r)}$  becomes negative, the MS- $n$  will not consider the RS- $r$  for coalition formation, thus RS- $r$  will not be included in the MS- $n$  ranking list,  $\iota_n$ .

- 3) Mobiles are only required to exchange their channel statistics in the uplink with the RSs willing to cooperate with them. Based on this information, RSs are able to rank their subset of MSs,  $S_r$ , by using the following utility function when diversity is enhanced

$$U_{rn\_diversity}(\eta_{\text{target}}) = P_{\text{circ}} \left( \frac{P_t(\eta_{\text{target}}) \|w_{\text{rs}}\|^2}{M_t} \right) - P_{\text{circ}} \left( \frac{P_t(\eta_{\text{target}}) \|w_{\text{ms}}\|^2}{M_t} \right), \quad (32)$$

For the capacity case, Eq. (32) may be re-written as follows:

$$U_{rn\_capacity}(T_{\text{target}}) = P_{\text{circ}} \left( \frac{P_t(T_{\text{target}}) \zeta_{\text{rs}}}{M_t} \right) - P_{\text{circ}} \left( \frac{P_t(T_{\text{target}}) \zeta_{\text{ms}}}{M_t} \right), \quad (33)$$

Equations (32) and (33) represent the difference in power expenditure between the RS- $r$  and the MS- $n$  when forming a virtual MIMO link. Thus, the larger the value of the utility the larger the power expenditure of the RS due to its better channel conditions in the reverse link when compared to the MS. Furthermore, the RS's preference list,  $\iota_r$ , is obtained by evaluating each of the elements in the  $S_r$  subset by Equations (32) or (33) when using spatial diversity or spatial multiplexing respectively. The elements of  $\iota_r$  are also sorted in descending order as the  $\iota_n$  case described previously in (31).

- 4) After the preference lists for MSs and RSs are obtained, Algorithm (1) [29] can be performed.

## V. ANALYSIS OF THE CONSEQUENCES IN PERFORMANCE OF MIMO SYSTEMS WHEN OPTIMIZING OVERALL CONSUMED POWER

In this section, we provide a theoretical analysis of the consequences that arise in terms of energy efficiency when overall power consumption is considered as an optimization metric rather than transmitted power. Hence, to show the effects on user performance, we analytically derive the statistics of the

**Algorithm 1:** College admission framework (CAF), after [29].

```

Initialization: All MSs must be operating in SIMO mode;
while There is an MS- $n$  wanting to form a MIMO link;
do
   $MS_r(h)$  is the highest ranked MS in the RS- $r$  preference list,  $\iota_r$ , to whom the RS- $r$  has not
  proposed yet;
  if RS- $r$  is contained in the  $MS_r(h)$ 's preference list; then
    if  $MS_r(h)$  is free; then
      | the  $MS_r(h)$  and the RS- $r$  become engaged;
    else
      |  $MS_r(h)$  is already engaged with a subset of RSs,  $\bar{S}_n \in R$ ;
      | if If adding the RS- $r$  to the  $MS_r(h)$  current subset of RSs,  $\bar{S}_n$ , provides energy savings;
      | then
      | | RS- $r$  becomes engaged;
      | end
      | if If adding the RS- $r$  to the  $MS_r(h)$  current subset of RSs,  $\bar{S}_n$ , does not provides extra
      | energy savings. Nevertheless,  $MS_r(h)$  prefers RS- $r$  to the RS- $t$  in its preference list,
      |  $\iota_r(h)$ , where RS- $t \in \bar{S}_n$ ; then
      | | RS- $r$  becomes engaged;
      | | RS- $t$  becomes free;
      | else
      | |  $MS_r(h)$  is deleted from the list of the RS- $r$ ,  $\iota_r$ ;
      | end
    end
  end
end

```

transmitted and overall consumed power when implementing spatial diversity or spatial multiplexing respectively. While these statistics can be obtained experimentally, we derive them in closed form.



### A. Spatial Diversity Approach

From Eq. (7), we know that the transmitted power of any signal,  $P_t$ , can be calculated by

$$P_t = \frac{P_r}{10^{\frac{-L(l_k)+X_\sigma}{10}}}, \quad (34)$$

Moreover, if we combine Eq. (11) with Eq. (34), we obtain the transmitted power for a MIMO user.

$$P_{t\_mimo} = \frac{\eta_{k\_mimo}\rho}{\sigma_{max}^2 10^{\frac{-L(l_k)+X_\sigma}{10}}}. \quad (35)$$

Given that, on average,  $\mathbf{E}\{\sigma_{max}^2\} \leq M_t \times M_r$  and  $X_\sigma = 0$  [4], this allows us to re-write the equation above as follows:

$$P_{t\_mimo} = \frac{\eta_{k\_mimo}\rho}{M_t \times M_r 10^{\frac{-L(l_k)}{10}}}. \quad (36)$$

To obtain the statistics for the transmitted power of a MIMO user,  $P_{t\_mimo}$ , we assume that the MSs are uniformly distributed in the cell. Therefore, for a circular cell of radius  $R$ , it is known that the probability distribution function (PDF) of the distance of any point from the center is [8]:

$$f_{l_k}(l_k) = \frac{2l_k}{R^2} \quad l_k \in [0, R] \quad (37)$$

In addition, from Eq. (8) we observe that pathloss is an element which is a function of distance, thus to derive its PDF we use the transformation of random variables. Thereby, we obtain the inverse relationship of the distance as a function of pathloss as follows:

$$l_k(L) = 10^{\left(\frac{L-a}{b}\right)}, \quad (38)$$

Hence, the pathloss PDF  $f_L(L)$  may be derived by

$$f_L(L) = \left\| \frac{dl_k}{dL} \right\| f_{l_k}(l_k(L)) \quad L \in [-\infty, a + b\log_{10}(R)] \quad [dB], \quad (39)$$

$$f_L(L) = \frac{2\log(10)}{bR^2} 10^{\frac{2(L-a)}{b}}. \quad (40)$$

After the statistics for the pathloss are obtained, we proceed to derive the PDF of the transmitted power. From Eq. (36), we are able to obtain the inverse relationship of the pathloss as a function of the transmitted power for a MIMO user,  $P_{t\_mimo}$ .

$$L(P_{t\_mimo}) = -10\log_{10} \left( \frac{\eta_{k\_mimo}\rho}{M_t M_r P_{t\_mimo}} \right), \quad (41)$$

Thus, the PDF of the transmitted power for a MIMO user can be obtained as follows:

$$f_{P_{t\_mimo}}(P_{t\_mimo}) = \left\| \frac{dL}{dP_{t\_mimo}} \right\| f_L(L(P_{t\_mimo})) \quad P_{t\_mimo} \in \left[ 0, \frac{\eta_{k\_mimo}\rho}{M_t M_r 10^{-\left(\frac{a+b\log_{10}(R)}{10}\right)}} \right], \quad (42)$$

$$f_{P_{t\_mimo}}(P_{t\_mimo}) = \frac{20}{bR^2 P_{t\_mimo}} 10^{\frac{-2}{b} \left( 10\log_{10} \left( \frac{\eta_{k\_mimo}\rho}{M_t M_r P_{t\_mimo}} \right) + a \right)}. \quad (43)$$

From Eq. (22), we see that the circuit consumed power,  $P_{\text{circ}}$ , depends of the transmitted power when converted to [dBm]. Thus, the inverse relationship of the transmitted power,  $P_{t\_mimo}$ , in function of the transmitted power in [dBm],  $P_{t\_mimo\_dBm}$ , for a MIMO user case is given by:

$$P_{t\_mimo}(P_{t\_mimo\_dBm}) = 1e^{-3} \times 10^{\frac{P_{t\_mimo\_dBm}}{10}}, \quad (44)$$

Thereby, the PDF of the transmitted power in [dBm],  $P_{t\_mimo\_dBm}$  is:

$$f_{P_{t\_mimo\_dBm}} = \left\| \frac{dP_{t\_mimo}}{dP_{t\_mimo\_dBm}} \right\| f_{P_{t\_mimo}}(P_{t\_mimo}(P_{t\_mimo\_dBm}))$$

$$P_{t\_mimo\_dBm} \in \left[ -\infty, 10\log_{10} \left( \frac{1e^3 \times \eta_{k\_mimo} \rho}{M_t M_r 10^{-(a+b\log_{10}(R))}} \right) \right], \quad (45)$$

$$f_{P_{t\_mimo\_dBm}} = \frac{2\log(10)}{bR^2} 10^{\frac{-2}{b} \left( 10\log_{10} \left( \frac{1e^3 \times \eta_{k\_mimo} \rho}{M_t M_r 10^{\frac{P_{t\_mimo\_dBm}}{10}}} \right) + a \right)} \quad (46)$$

Moreover, it can be observed that the input of  $P_{\text{circ}}$  in Eq. (18) is the transmitted power for each antenna in [dBm]. Thereby, assuming that the total transmitted power for a MIMO user,  $P_{t\_mimo}$ , is divided evenly between each antenna as it was proposed for this derivation, the PDF of the transmitted power per antenna in [dBm],  $P_t^*$ , is given by:

$$f_{P_t^*} = \frac{2\log(10)}{bR^2} 10^{\frac{-2}{b} \left( 10\log_{10} \left( \frac{1e^3 \times \eta_{k\_mimo} \rho}{M_t^2 M_r 10^{\frac{P_t^*}{10}}} \right) + a \right)} P_t^* \in \left[ -\infty, 10\log_{10} \left( \frac{1e^3 \times \eta_{k\_mimo} \rho}{M_t^2 M_r 10^{-(a+b\log_{10}(R))}} \right) \right], \quad (47)$$

Finally, we derive the inverse relationship of the transmitted power per antenna in [dBm] as a function of the circuit consumed power in the reverse link by combining Eqs. (18) and (22) as follows:

$$P_t^*(P_{\text{mimo\_diversity}}) = \begin{cases} \frac{\gamma+A-2}{0.005} & 14 \geq P_t^*, \\ \frac{4\gamma+(A-\frac{3P_{BB}}{4})-1.2}{0.117} & 17 \geq P_t^* > 14, \\ \frac{2\gamma+(A-P_{BB})-1.2}{0.117}, & 20 \geq P_t^* > 17, \\ \frac{\gamma+A-1.2}{0.117} & 24 \geq P_t^* > 20. \end{cases} \quad (48)$$

where  $\gamma = \frac{P_{\text{mimo\_diversity}}}{M_t}$ . Hence, by using the transformation of random variables, the PDF of the circuit consumed power in the reverse link for a MIMO user is shown below:

$$f_{P_{\text{mimo\_diversity}}} = \begin{cases} \frac{363\log(10)}{bR^2M_t} 10^{-\frac{2}{b}} \left( 10\log_{10} \left( \frac{1e^3 \times \eta_k \text{ mimo } \rho}{z_{10}^{\frac{2+A-2}{0.05}}} \right) + a \right) & P_{\text{mimo\_diversity}} \in [0, M_t(2 + 0.005Z1 - A)], \\ \frac{68\log(10)}{bR^2M_t} 10^{-\frac{2}{b}} \left( 10\log_{10} \left( \frac{1e^3 \times \eta_k \text{ mimo } \rho}{z_{10}^{\frac{4\gamma+A-0.75P_{BB}-1.2}{1.17}}} \right) + a \right) & P_{\text{mimo\_diversity}} \in [M_t(2 + 0.005Z1 - A), M_t(\frac{1.2+0.117Z1-Z2}{4})], \\ \frac{34\log(10)}{bR^2M_t} 10^{-\frac{2}{b}} \left( 10\log_{10} \left( \frac{1e^3 \times \eta_k \text{ mimo } \rho}{z_{10}^{\frac{2\gamma+A-P_{BB}-1.2}{1.17}}} \right) + a \right) & P_{\text{mimo\_diversity}} \in [M_t(\frac{1.2+0.117Z1-Z2}{4}), M_t(\frac{1.2+0.117Z1-Z3}{2})], \\ \frac{17\log(10)}{bR^2M_t} 10^{-\frac{2}{b}} \left( 10\log_{10} \left( \frac{1e^3 \times \eta_k \text{ mimo } \rho}{z_{10}^{\frac{2+A-1.2}{1.17}}} \right) + a \right) & P_{\text{mimo\_diversity}} \in [M_t(\frac{1.2+0.117Z1-Z3}{2}), M_t(1.2 + 0.117Z1 - A)]. \end{cases} \quad (49)$$

where  $Z = M_t^2 M_r$ ,  $Z1 = 10\log_{10} \left( \frac{1e^3 \times \eta_k \text{ mimo } \rho}{M_t^2 M_r 10^{-(a+b\log_{10}(R))}} \right)$ ,  $Z2 = A - (0.75 \times P_{BB})$  and  $Z3 = A - P_{BB}$ .

Finally, by integrating the PDFs of the transmitted and circuit consumed power over their respective ranges, we obtain the cumulative distribution functions (CDFs) for transmitted and circuit consumed power, which are shown in Fig. 5(a) and 5(b), respectively. In addition, we also find the CDFs by simulation to compare them with our theoretical derivations. Moreover, as an example we consider SIMO and MIMO users with three and six antennas. Furthermore, we require the users independent of SIMO or MIMO mode to achieve the same target SNR,  $\eta_{\text{target}}$ , in order to make fair comparisons in terms of power expenditure. It should be noticed that for obtaining the statistics of the overall consumed power for the SIMO case, it follows a similar procedure as the one shown for the MIMO user case. For the required values to evaluate the statistics and perform the simulations, we consider the values shown in Table I. These results are discussed further in Subsection V-C below.

### B. Spatial Multiplexing Approach

For the following derivations, we use Shannon's capacity formula for ease of analysis and without loss of generality. Thus, Eq. (26) can be re-written as follows:

$$T_{k\_capacity} = \sum_{i=1}^J \log_2(1 + \eta_{i\_SC}) = \sum_{i=1}^J \log_2\left(1 + \frac{P_r \zeta_i \sigma_i}{M_t \rho}\right), \quad (50)$$

Moreover, if we assume equal gain conditions between the multiple parallel SISO channels  $\zeta_i = 1$ ,  $\mathbf{E}\{\|\mathbf{H}\|_F^2\} = M_r M_t = J \sigma_i$  [4]. The previous Eq. (50) may be re-written in the following way:

$$T_{k\_capacity} = \sum_{i=1}^J \log_2(1 + \eta_{i\_SC}) = J \log_2\left(1 + \frac{P_r M_r}{J \rho}\right), \quad (51)$$

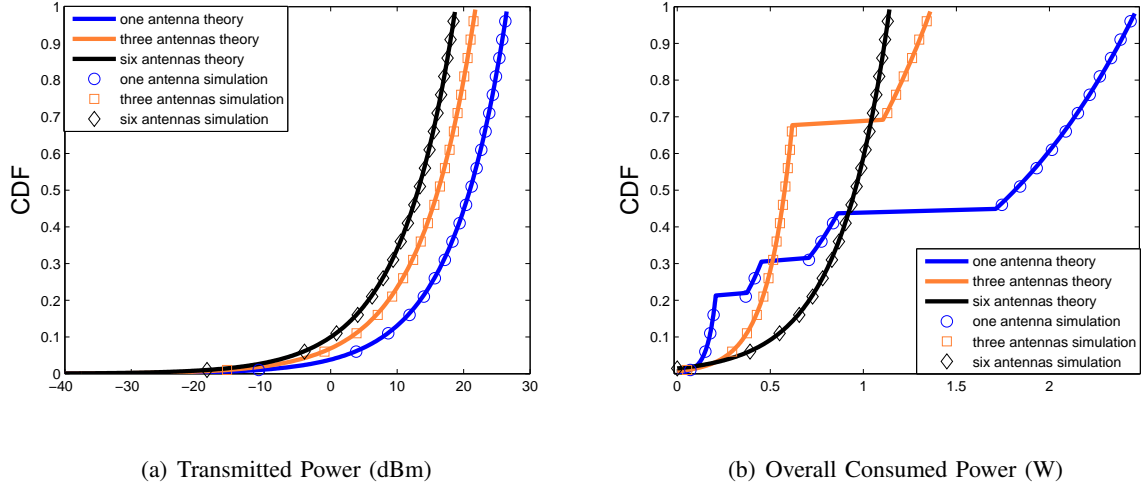


**Fig. 5** User performance differences, when enhancing diversity and optimizing transmitted 5(a) and overall consumed power 5(b) respectively

Thus, by combining Eq. (34) and Eq. (51), we obtain the required transmitted power as:

$$P_t = \frac{\beta}{M_r 10^{\frac{-L(d_k)}{10}}}, \quad (52)$$

where  $\beta = (2^{\frac{T_{k\_capacity}}{J}} - 1)J\rho$ . Moreover, to obtain the statistics of the transmitted power  $P_t$ , we assume that the MSs are uniformly distributed over the cell. Moreover, from Eq. (52) we obtain the inverse relationship of the pathloss in function of the transmitted power.

$$L(P_t) = -10\log_{10}\left(\frac{\beta}{M_r P_t}\right), \quad (53)$$

Thus, by using a similar approach as the one used in Eq. (42), the PDF of the transmitted power may be obtained, as:

$$f_{P_t} = \frac{20}{R^2 b P_t} 10^{\frac{-2}{b}(a + 10\log_{10}(\frac{\beta}{M_r P_t}))} P_t \in \left[0, \frac{\beta}{M_r 10^{-(\frac{a + b\log_{10}(R)}{10})}}\right], \quad (54)$$

Furthermore, we require to obtain the transmitted power in [dBm]. Thus, the inverse relationship of the transmitted power,  $P_t$ , as function of the transmitted power in [dBm],  $P_{t\_dBm}$ , is given by:

$$P_t(P_{t\_dBm}) = 1e^{-3} 10^{\frac{P_{t\_dBm}}{10}}, \quad (55)$$

Thereby, by using a similar approach as the used in Eq. (45), we derive the PDF of the transmitted power in [dBm] as follows.

$$f_{P_{t\_dBm}} = \frac{20\log(10)1^{-3}}{R^2b} 10^{\frac{-2}{b} \left( a + 10\log_{10} \left( \frac{\beta}{1e^{-3}M_r10^{\frac{P_{t\_dBm}}{10}}} \right) \right)} P_{t\_dBm} \in \left[ -\infty, 10\log_{10} \left( \frac{1e^3 \times \beta}{M_r10^{-\left(\frac{a+b\log_{10}(R)}{10}\right)}} \right) \right], \quad (56)$$

As in the diversity case, we should observe that in order to compute the circuit consumed power  $P_{\text{circ}}$ , Eq(22), we require the transmitted power per antenna. Thus, assuming that the transmitted power is divided evenly over all the antennas, the PDF of the transmitted power per antenna in [dBm] is:

$$f_{P_t^*} = \frac{20\log(10)}{R^2b} 10^{\frac{-2}{b} \left( a + 10\log_{10} \left( \frac{\beta}{M_r M_t 1e^{-3}10^{\frac{P_t^*}{10}}} \right) \right)} P_t^* \in \left[ -\infty, 10\log_{10} \left( \frac{1e^3 \times \beta}{M_t M_r 10^{-\left(\frac{a+b\log_{10}(R)}{10}\right)}} \right) \right], \quad (57)$$

Finally, we derive the inverse relationship of the transmitted power per antenna in [dBm] as a function of the circuit consumed power in the reverse link by combining Eqs. (19) and (22) as shown:

$$P_t^*(P_{\text{mimo\_capacity}}) = \begin{cases} \frac{\gamma_1 + A - 2}{0.005} & 14 \geq P_t^*, \\ \frac{4\gamma_1 + (A - \frac{3P_{BB}}{4}) - 1.2}{0.117} & 17 \geq P_t^* > 14, \\ \frac{2\gamma_1 + (A - P_{BB}) - 1.2}{0.117}, & 20 \geq P_t^* > 17, \\ \frac{\gamma_1 + A - 1.2}{0.117} & 24 \geq P_t^* > 20. \end{cases} \quad (58)$$

where  $\gamma_1 = \frac{P_{\text{mimo\_capacity}}}{M_t}$ . Moreover, by using the transformation of random variables, the PDF of the circuit consumed power is shown below:

$$f_{P_{\text{mimo\_capacity}}} = \begin{cases} \frac{363\log(10)}{bR^2M_t} 10^{\frac{-2}{b} \left( 10\log_{10} \left( \frac{1e^3\beta}{M_t M_r 10^{\frac{\gamma_1 + A - 2}{0.05}}} \right) + a \right)} P_{\text{mimo\_capacity}} \in [0, M_t(2 + 0.005Z1 - A)], \\ \frac{68\log(10)}{bR^2M_t} 10^{\frac{-2}{b} \left( 10\log_{10} \left( \frac{1e^3\beta}{M_t M_r 10^{\frac{4\gamma_1 + A - 0.75P_{BB} - 1.2}{1.17}}} \right) + a \right)} P_{\text{mimo\_capacity}} \in [M_t(2 + 0.005Z1 - A), M_t(\frac{1.2 - 0.117Z1 - Z2}{4})], \\ \frac{34\log(10)}{bR^2M_t} 10^{\frac{-2}{b} \left( 10\log_{10} \left( \frac{1e^3\beta}{M_t M_r 10^{\frac{2\gamma_1 + A - P_{BB} - 1.2}{1.17}}} \right) + a \right)} P_{\text{mimo\_capacity}} \in [M_t(\frac{1.2 - 0.117Z1 - Z2}{4}), M_t(\frac{1.2 + 0.117Z1 - Z3}{2})], \\ \frac{17\log(10)}{bR^2M_t} 10^{\frac{-2}{b} \left( 10\log_{10} \left( \frac{1e^3\beta}{M_t M_r 10^{\frac{\gamma_1 + A - 1.2}{1.17}}} \right) + a \right)} P_{\text{mimo\_capacity}} \in (M_t(\frac{1.2 + 0.117Z1 - Z3}{2}), M_t(1.2 + 0.117Z1 - A)]. \end{cases} \quad (59)$$

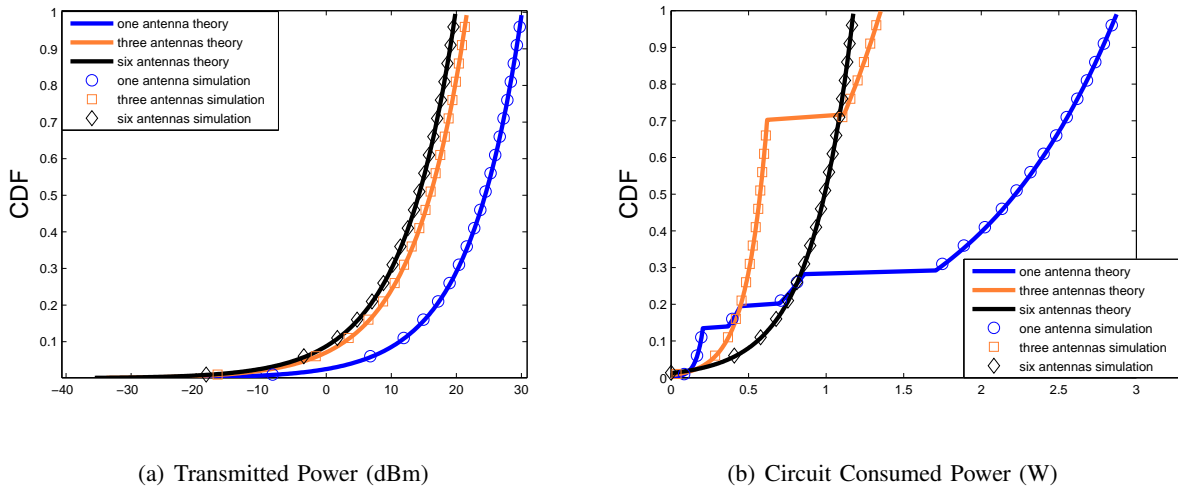


**Fig. 6** User performance differences, when implementing spatial multiplexing and optimizing transmitted power 6(a) and overall consumed power 6(b) respectively

where  $Z1 = 10\log_{10}\left(\frac{1e^3\beta}{M_r M_t 10^{-\left(\frac{a+b\log_{10}(R)}{10}\right)}}\right)$ ,  $Z2 = A - (0.75 \times P_{BB})$  and  $Z3 = A - P_{BB}$ .

Finally as in the diversity case, by integrating the PDFs of the transmitted and circuit consumed power over their respective ranges, we obtain the cumulative distribution functions (CDFs) for transmitted and circuit consumed power, which are shown in Fig. 6(a) and 6(b) respectively. In addition, we also find the CDFs by simulation to compare them with our theoretical derivations. As an example, we consider SIMO and MIMO users carrying three and six antennas. Furthermore, we make the users independently of SIMO or MIMO to achieve the same transmission rate, in order to make fair comparisons in terms of power expenditure. To evaluate the statistics and perform the simulations, we consider the values shown in Table I.

### C. Analysis

From Figs. 5(a) and 6(a), it is easy to see that increasing the number of antennas provides power savings at all percentiles of the CDF when only transmitted power is optimized. However, this trend does not remain the same when optimizing circuit power consumption. In Fig. 5(b) in the case of diversity, we see that the SIMO curve intersects the MIMO curves when transmitting with three and six antennas at the 30<sup>th</sup> and 45<sup>th</sup> percentile respectively. Moreover, for the capacity case in Fig. 6(b), we see that the

SIMO curve intersects the MIMO curves when transmitting with three and six antennas at the 20<sup>th</sup> and 28<sup>th</sup> percentile respectively. This intersection point represents that in the diversity case, SIMO is more power efficient for 30% and 45% of the users in the cell when compared to MIMO when transmitting with three and six antennas respectively. The same relation holds for the spatial multiplexing case. This is because the MSs are able to experience better transmission conditions, when they are close to the BS. Thus, turning on the RF transmitter and the BB module of the relay stations is less power efficient than transmitting with only one antenna. Nevertheless, as the users get close to the cell edge increasing the number of transmit antennas tends to be an energy efficient solution when circuit power consumption is optimized. This fact can be seen from Figs. 5(b) and 6(b), since as the number of antennas increases, it allows the three and six antennas curves to converge faster to the tail of the distribution. Our analysis in this section will be useful to understand the performance of the proposed framework in Section VII.

## VI. COMPARISON SCHEMES AND SIMULATION SCENARIO

To evaluate the performance of our proposal, we describe four distributed relay selection algorithms which allow MSs and RSs to cooperate to form MIMO coalitions with the purpose of reducing the energy consumption in the reverse link. In addition, a baseline scheme is presented where all MSs transmit on their own in SIMO mode. Finally, a centralized global optimum approach which is coordinated from the BS and based on an exhaustive search is presented. For all the described methods, the communication between the MSs and RSs is made through the cooperative link. Thus, the subset of RSs willing to cooperate with the MS- $n$  is limited by the range of the cooperative link, which naturally limits the complexity of the relay selection.

1) *Minimum Relaying Hop (MRH) Path Loss Selection scheme:* In [30], the authors propose a relay selection method as a function of path loss. Hence, the best RS for coalition formation is the one with the least path loss to the MS, this method always chooses the RS with the most energy efficient cooperative link.

$$RS_c = \operatorname{argmin}\{d_{nr}^k\} \quad (60)$$

From (60), it should be noticed that for performing the RS selection it is just required to know the channel statistics of the cooperative link.

2) *Best Worst (BW) Channel Selection scheme:* The BW method considers the quality of the cooperative and the reverse link of each RS. This is because both links have a direct influence on the total consumed energy for forming the virtual MIMO link. In [30], the best worst channel is used in which

the relay whose worse channel is the best is selected:

$$\operatorname{argmin}\left\{\|G_r, \frac{1}{d_{nr}^\kappa}\|\right\}, \quad (61)$$

where  $G_r = \|\mathbf{h}_r\|_F^2 10^{\frac{-L(l_r)+X_\sigma}{10}}$  represents the channel path gain between the RS- $r$  and the BS, and  $l_r$  defines the distance between the  $r$ -th RS and the BS.

3) *Stable Marriage (SMI) scheme*: In [21], we present a distributed RS selection algorithm which is based on the stable marriage process. This method, as in the BW channel selection scheme, requires the channel statistics from the RSs in the reverse and cooperative link plus the channel statistics of the MSs in the reverse link. Thereby, each MS and RS is able to rank its respective candidates for coalition formation. It should be noticed that the SMI method has the same limitation as MRH and BW methods in that each MS is only able to select one RS.

4) *SIMO transmission*: We implement a baseline scheme, where all the MSs in the network transmit in SIMO mode.

5) *CAF scheme*: This scheme implements our RS selection method described in Section IV.

6) *Centralized optimum scheme*: A centralized global optimum scheme, based on an exhaustive search approach, is presented. Thus, the BS collects the required channel statistics from RSs and MSs in order to form optimal coalitions. We implement this centralized approach with the aim of finding the price of anarchy for our proposed scheme. The *price of anarchy* is computed as the difference in performance between a centralized and a distributed approach.

#### A. Simulation scenario

Monte Carlo simulations are performed using the parameters presented in Table I. This is done to compare the performance of our method with the schemes presented above. The simulation is comprised of a single cell with the MSs and RSs distributed uniformly over the cell area. The cell is served by an omnidirectional BS. Moreover, the system is noise limited, hence each coalition transmits in an independent RB to avoid co-channel interference. For the case when diversity is enhanced, we assume that all the *users* (SIMO or MIMO), independent of their distance to the BS try to achieve the same target SNR,  $\eta_{\text{target}}$ . In the case when spatial multiplexing is used we assume that all the users in the network aim to achieve the same data rate,  $T_{\text{target}}$ .

## VII. RESULTS

From the simulations, we generate the cumulative distribution functions (CDFs), and the graphs that illustrate the performance in terms of *overall power expenditure* for the schemes presented at the start



**TABLE I** Simulation parameters.

Parameter	Value
MSs per macro-cell, $N$	20
RSs per macro-cell, $R$	95
Number of antennas at the receiver, $M_r$	6
Cell radius	150m
Number of available RBs, $X$	20
Number of cells, $D$	1
Subcarriers per RB, $k_{sc}$	12
Symbol rate per subcarrier, $\varrho_s$	15ksps
$P_{Tx}$	31.8dBm
$P_{con}$	23.8dBm
$P_{BB}$	11.7dBm
Maximum user transmit power	24dBm
Shadowing, Std. Dev., $\sigma$	3dB
$\eta_{target}$	17dB
$T_{target}$	910 kbps
$\varepsilon$ for 17dB SNR	$4.5 \frac{\text{bits}}{\text{symbol}}$
$\kappa$	3.5
Pathloss constant, $a$	15.3
Pathloss constant, $b$	37.6

of this section.

When diversity is enhanced in Fig. 7, we show the overall consumed power at different distances from the BS, where all the users in the cell aim to achieve the same target SNR. We observe that the distributed and centralized approaches exhibit a similar performance when compared to the baseline method at close distances from the BS (up to 75 m). This is because as mentioned in the analysis presented in Section V-A, MSs experience good transmission conditions close to the cell center. Thus, turning on the BB and RF module of the RSs becomes less power efficient than transmitting with only one antenna. Conversely, when channel conditions are no longer so beneficial (e.g., after 75 m), we see that as the MSs move away from the BS, the increase from one to a higher number of transmit antennas allows the MS to obtain potential energy savings. Furthermore, from the analysis shown in Section V-A and the results presented Fig. 7, we can confirm that, when circuit power consumption is optimized and spatial diversity is enhanced, by increasing the number of antennas the obtained power savings are more visible at cell

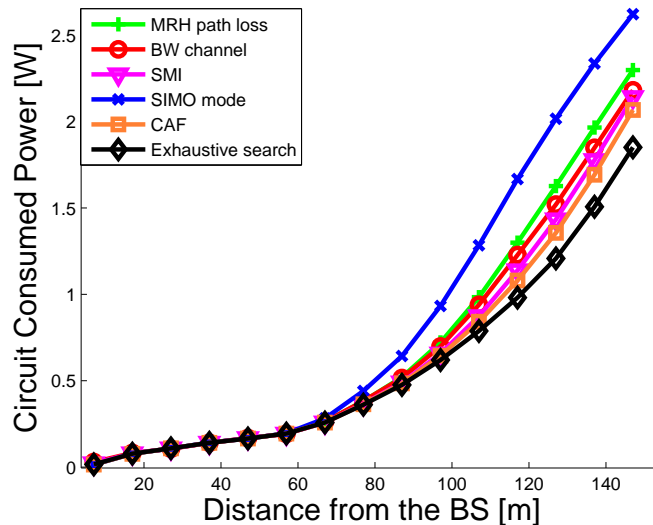


**Fig. 7** User circuit consumed power against distance from the BS.

edge than at the cell center. In Fig. 8, the system energy efficiency, given by Equation (28), is evaluated. Notice that at the 50<sup>th</sup> percentile the CAF scheme is more energy efficient compared to the benchmark, the MRH pathloss, the BW channel, and the SMI framework with improvements of 58%, 15%, 10% and 5% respectively. Nevertheless, the CAF scheme has losses of 10% compared to the centralized global optimum scheme. These losses are tolerable in practice due to the significant reductions in complexity for the CAF method compared to the centralized optimum scheme: this is discussed further at the end of this section. Moreover, the better performance in energy efficiency terms for the CAF and centralized optimum when compared to the other distributed approaches can be easily understood as a direct consequence of the bigger number of antenna elements than can be involved in the coalition.

When spatial multiplexing is used, we aim to obtain gains in energy efficiency by dividing the total data rate requirements between the elements forming the virtual MIMO link. Thereby, as in the diversity case it can be observed from Fig. 9 that the most of the power savings due to coalition formation are observed at the cell border. This is because, it is more power efficient to deliver high transmission rates for SIMO users who close to the BS than when close to the cell edge due to the improved propagation conditions. Thus, using a lower modulation order for transmitting from each antenna in a coalition when close to the cell edge becomes more power efficient than using a single transmitter. Hence, from the results shown in Section V-B and Fig. 9, it can be understood that increasing the number of transmit antennas to split the total rate requirement among the transmitters by implementing spatial multiplexing

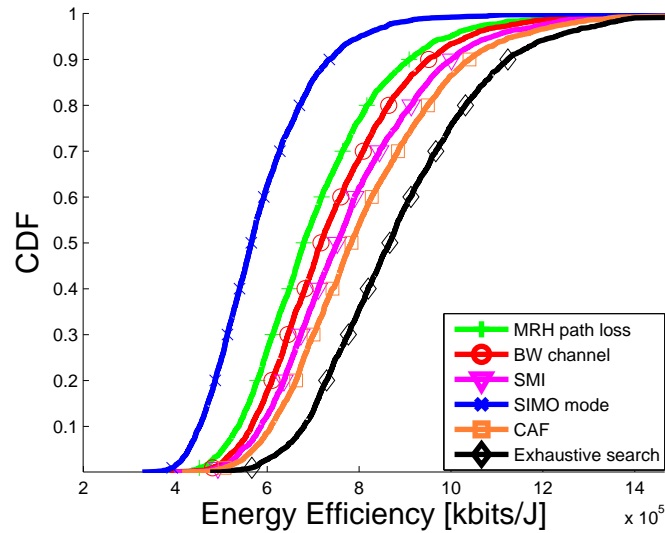


**Fig. 8** System CDF energy efficiency.

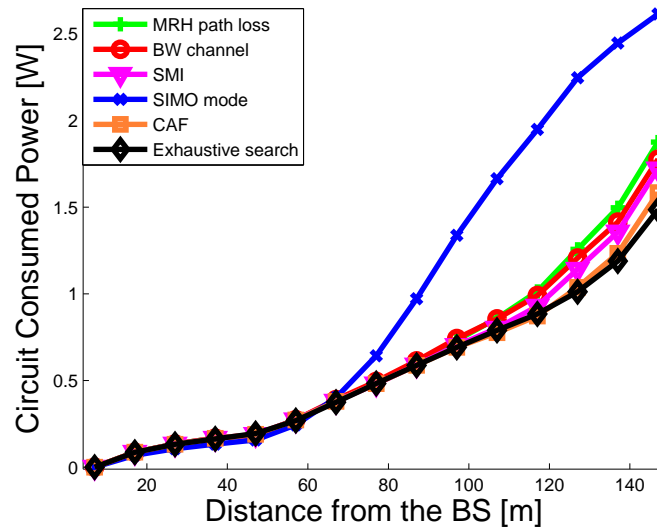


**Fig. 9** User circuit consumed power against distance from the BS.

is more power efficient in terms of overall power consumption at the cell border than at the cell center.

Finally, in Fig. 10 we show the performance in terms of energy efficiency for the approaches presented in Section VI when spatial multiplexing is implemented. We find that the centralized global optimum is 2% more energy efficient when contrasted to the CAF. Moreover, when comparing the CAF with the other distributed approaches we see that the CAF method has improvements of 14%, 9%, 5%, and 91%

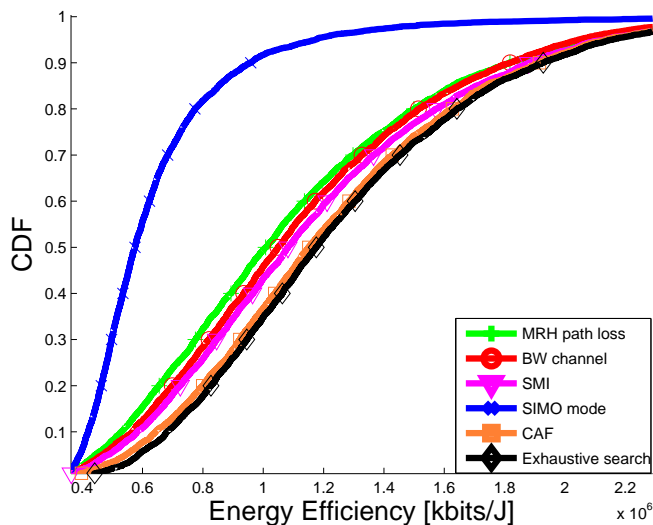


**Fig. 10** System energy efficiency when enhancing capacity.

over MRH, BW, SMI, and the baseline SIMO mode respectively. Thereby, we can confirm that increasing the number of antennas in order to use a lower modulation order results in an energy efficient solution for the network.

To conclude our comparison, we discuss the complexity of the centralized global optimum approach compared with the proposed CAF method. On one hand, for the CAF method each MS- $n$  in the system has to evaluate each RS in its preferred subset of suitable candidates,  $S_n$ , by using Eqs. (29) or (30) depending on whether diversity or capacity are enhanced. Furthermore, each RS- $r$  evaluates its preferred subset  $S_r$  of RSs by using Eqs. (32) or (33). Thus, arithmetic operations with a complexity of  $|S_n|^2$  and  $|S_r|^2$  are performed by the system when candidate MSs or RS are ranked respectively, where  $|\cdot|$  defines the cardinality of the subset. If we assume that  $R \gg N$ , the complexity of the candidate ranking process is bounded by the number of RSs in the system rather than by the number of MSs. Thereby, this will allow us to upper bound the complexity of the candidate ranking by  $|S_n|^2$  operations. Moreover, forming the MS's preference list,  $\iota_n$ , (31) requires a sorting operation which induces a complexity of  $|S_n|\log(|S_n|)$  operations. Finally, the complexity of the decision making Algorithm (1) can be upper bounded by a binary search operation which requires a complexity of  $\log(|S_n|)$  operations. Therefore, the dominant factor which determines the CAF scheme complexity will be the one with the largest exponent, thus the complexity of the method will be upper bounded by order  $|S_n|^2$  operations. On the other hand, the centralized global optimum scheme is based on enumerating all possible alternatives for virtual MIMO

coalition formation between the MS- $n$  and its preferred subset of candidate RSs,  $S_n$ . This is done with the purpose of finding the optimal number of transmit antennas that would minimize the overall power consumption in the reverse link. Therefore, to guarantee that a given feasible solution is optimal, the solution should be compared with any other feasible solutions. In general, an exhaustive search approach, when the number of elements is discrete, is considered  $\mathcal{NP}$ -complete [31]. A notable characteristic of  $\mathcal{NP}$ -complete problems is that the required time to solve the problem increases very quickly as the size of the problem grows [31]. To implement the exhaustive search scheme, each MS in the system will evaluate the total number of possible combinations in its preferred subset of candidate RSs,  $S_n$ . Hence, the total number of possible combinations is computed by  $\sum_{k=1}^{|S_n|} \binom{|S_n|}{k}$ , where  $\binom{|S_n|}{k} = \frac{|S_n|!}{k!(|S_n|-k)!}$ . Moreover, each combination is evaluated by Eqs. (20) or (21) depending if diversity or capacity are enhanced respectively. Thus, it induces a complexity of  $(\sum_{k=1}^{|S_n|} \binom{|S_n|}{k})^2$  for the system. In addition the complexity of both presented methods (exhaustive search and CAF) increases linearly with the number of MSs in the system,  $N$ . Finally, big  $\mathcal{O}$  notation is used to describe the growth rate of the both schemes. Hence, the exhaustive search method has a complexity of  $\mathcal{O}(N \times (\sum_{k=1}^{|S_n|} \binom{|S_n|}{k})^2)$  which is a higher order complexity when compared to the complexity of  $\mathcal{O}(N \times |S_n|^2)$  for the CAF scheme. Furthermore, Fig. 11 shows how the complexity of the system changes for both methods as the number of RSs increases in the system. It can be easily seen that as the number of RSs increases, the computational complexity of the exhaustive search increases exponentially, therefore it may not be a suitable solution for being implemented in real time systems.

## VIII. CONCLUSIONS

In this paper, we considered a low complexity virtual MIMO coalition formation algorithm, which is based on game theory. Our proposed framework allows MSs to select the most suitable RSs providing the most power savings in the network. Thereby, we studied energy efficient coalition formation by using the concepts of diversity and spatial multiplexing, respectively. We have shown analytically and by simulation that increasing the number of transmit antennas is a more energy efficient solution for users close to the cell edge rather than for cell center users, when overall terminal power consumption is optimized. Furthermore, by performance comparisons we have proven that the proposed coalition formation algorithm is more energy efficient compared to the benchmark, the MRH pathloss, the BW channel, and the SMI framework with improvements of 58%, 15%, 10% and 5% for the spatial diversity case. When implementing spatial multiplexing the CAF method has improvements of 14%, 9%, 5%, and 91% over MRH, BW, SMI, and the baseline SIMO mode. It experiences only small performance

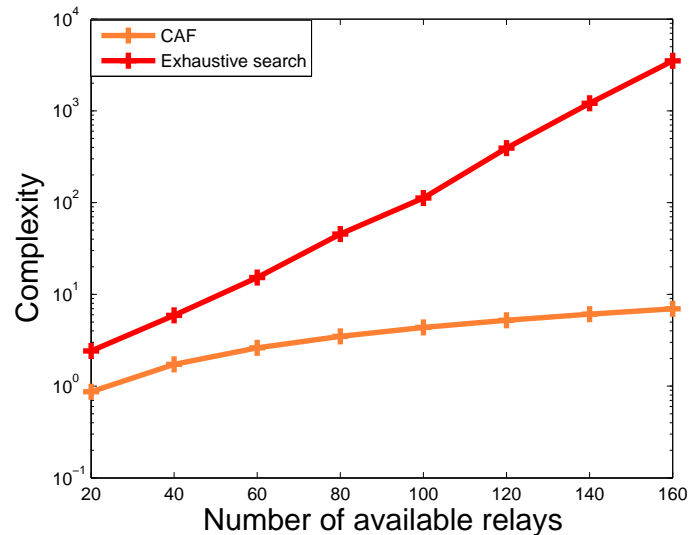


**Fig. 11** Complexity of the centralized optimum approach compared to the CAF method.

losses of 10% and 2% when compared to an exhaustive search approach when implementing diversity and spatial multiplexing respectively. In addition, we presented a complexity analysis, showing that the complexity of our proposed method increases linearly as the number of RSs grows in the network. This is a much lower complexity when compared to the exponential growth of the exhaustive search scheme. Thus, our proposed game theory framework achieves a similar performance compared to a centralized scheme with a much lower order complexity. Hence, it may be a suitable energy efficient solution for practical applications.

## REFERENCES

- [1] R. Vaca, J. Thompson, and V. Ramos, “Non-cooperative uplink interference protection framework for fair and energy efficient Orthogonal Frequency Division Multiple Access networks,” *IET Communications*, vol. 7, no. 18, pp. 2015–2025, 2013.
- [2] C. Han, T. Harrold, S. Armour, I. Krikidis, S. Videv, P. M. Grant, H. Haas, J. Thompson, I. Ku, C.-X. Wang, T. A. Le, M. Nakhai, J. Zhang, and L. Hanzo, “Green radio: radio techniques to enable energy-efficient wireless networks,” *IEEE Communications Magazine*, vol. 49, no. 6, pp. 46–54, 2011.
- [3] R. Wang, J. Thompson, H. Haas, and P. Grant, “Sleep mode design for green base stations,” *IET Communications*, vol. 5, no. 18, pp. 2606–2616, 2011.
- [4] A. Paulraj, R. Nabar, and D. Gore, *Introduction to space-time wireless communications*, C. U. Press, Ed. Cambridge University Press, Jul. 2003.
- [5] J. Jiang, M. Dianati, M. Imran, and Y. Chen, “Energy efficiency and optimal power allocation in virtual-MIMO systems,” in *Proceedings of the IEEE 76th Vehicular Technology Conference*, Sep. 2012, pp. 1–6.

- [6] S. Sesia, I. Toufik, and M. Baker, *LTE-The UMTS Long Term Evolution From Theory to Practice*, 1st ed., C. Wiley, Ed. Wiley, Chichester, 2009.
- [7] Z. Han, D. Niyato, T. Başar, and A. Hjørungnes, *Game Theory in Wireless and Communication Networks*. Cambridge University Press, Oct. 2012.
- [8] S. Hussain, A. Azim, and J. Park, “Energy efficient virtual MIMO communication for wireless sensor networks,” *Telecommunication Systems*, vol. 42, no. 1-2, pp. 139–149, 2009.
- [9] W. Saad, Z. Han, M. Debbah, A. Hjørungnes, and T. Basar, “Coalitional game theory for communication networks,” *Signal Processing Magazine, IEEE*, vol. 26, no. 5, pp. 77–97, 2009.
- [10] F. Pantisano, M. Bennis, W. Saad, R. Verdone, and M. Latva-aho, “Coalition formation games for femtocell interference management: A recursive core approach,” in *Wireless Communications and Networking Conference (WCNC), 2011 IEEE*, 2011, pp. 1161–1166.
- [11] A. Ibrahim, A. Sadek, W. Su, and K. Liu, “Cooperative communications with relay-selection: when to cooperate and whom to cooperate with?” *IEEE Transactions on Wireless Communications*, vol. 7, no. 7, pp. 2814–2827, 2008.
- [12] E. Larsson and E. Jorswieck, “Competition versus cooperation on the MISO interference channel,” *Selected Areas in Communications, IEEE Journal on*, vol. 26, no. 7, pp. 1059–1069, 2008.
- [13] R. Vaca, J. Thompson, E. Altman, and V. Ramos, “A game theory framework for a distributed and energy efficient bandwidth expansion process,” in *To appear in the Proceedings of the INFOCOM Workshop on Green Cognitive Communications and Computing Networks*, May 2014.
- [14] K. Yazdi, E. Gammal, and P. Schitner, “On the desing of cooperative transmission schemes,” in *Allerton Conference on Communications, Control and Computing*, 2003.
- [15] N. Jindal, U. Mitra, and A. Goldsmith, “Capacity of ad-hoc networks with node cooperation,” in *International Symposium on Information Theory (ISIT) 2004.*, 2004, p. 271.
- [16] S. Cui, A. Goldsmith, and A. Bahai, “Energy efficiency of MIMO and Cooperative MIMO Techniques in Sensor Networks,” *IEEE Journal on Selected Areas in Communications*, vol. 22, no. 6, pp. 1089–1098, Aug 2004.
- [17] S. Hussain, A. Azim, and J. Park, “Energy efficient virtual MIMO communication for wireless sensor networks,” *Telecommunication Systems*, vol. 42, no. 1-2, pp. 139–149, 2009.
- [18] Z. Han *et al.*, *Game Theory in Wireless and Communication Networks*, C. U. Press, Ed. Cambridge University Press, Oct. 2012.
- [19] Z. Han and R. Liu, “Fair multiuser channel allocation for OFDMA networks using Nash bargaining solutions and coalitions,” *IEEE Transactions on Communications*, vol. 53, no. 8, pp. 1366–1376, 2005.
- [20] W. Saad, Z. Han, and M. Debbah, “A distributed coalition formation framework for fair user cooperation in wireless networks,” *IEEE Transactions on Wireless Communications*, vol. 8, no. 9, pp. 4580–4593, Sep. 2009.
- [21] R. Vaca, E. Altman, J. Thompson, and V. Ramos, “A stable marriage framework for distributed virtual MIMO coalition formation,” in *Proceedings of the 24th Annual IEEE International Symposium on Personal Indoor and Mobile Radio Communications (PIMRC)*, Sep. 2013, pp. 2722–2727.
- [22] H. Burchardt *et al.*, “Uplink interference protection and scheduling for energy efficient OFDMA networks,” *EURASIP Journal on Wireless Communications and Networks*, vol. 2012, no. 180, p. 19, 2012.
- [23] Q. Li, G. Li, W. Lee, M. il Lee, D. Mazzarese, B. Clerckx, and Z. Li, “MIMO techniques in WiMAX and LTE: a feature overview,” *IEEE Communications Magazine*, vol. 48, no. 5, pp. 86–92, 2010.
- [24] T. Cover and J. Thomas, *Elements of Information Theory*, Wiley, Ed. Wiley-Interscience, Aug. 1991.

- [25] A. Jensen, M. Lauridsen, P. Mogensen, T. Srensen, and P. Jensen, "LTE UE power consumption model for system level energy and performance optimization," in *Proceedings of the IEEE 76th Vehicular Technology Conference*, Sep. 2012, pp. 1–6.
- [26] K. Bobae, K. Cholho, and L. Jongsoo, "A dual-mode power amplifier with on-chip switch bias control circuits for LTE handsets," *IEEE Transactions on Circuits and Systems*, vol. 58, no. 12, pp. 857–861, 2011.
- [27] D. Gale and M. Sotomayor, "Some remarks on the stable matching problem," *Discrete Applied Mathematics*, vol. 11, no. 3, pp. 223 – 232, 1985.
- [28] K. Iwama, , and S. Miyazaki, "A survey of the stable marriage problem and its variants," in *Proceedings of the International Conference on Informatics Research for Development of Knowledge Society Infrastructure*, Jan 2008, pp. 131–136.
- [29] D. Gale and L. S. Shapley, "College admissions and the stability of marriage," *The American Mathematical Monthly*, vol. 69, no. 1, pp. 9 – 15, 1962.
- [30] V. Sreng *et al.*, "Relayer selection strategies in cellular networks with peer-to-peer relaying," in *Proceedings of the IEEE 58th Vehicular Technology Conference*, Oct. 2003, pp. 1949–1953.
- [31] Z. Han and K. J. R. Liu, *Resource Allocation for Wireless Networks*, C. U. Press, Ed. Cambridge University Press, Jul. 2008.